Modeling Far-Field RF Sheaths in Alcator C-Mod

D. A. D'Ippolito and J. R. Myra

Lodestar Research Corporation,
Boulder, Colorado, USA

R. Ochoukov and D. G. Whyte

MIT Plasma Science and Fusion Center,
Cambridge, MA, USA

June, 2013

For the Proceedings of the 20ᵗʰ Topical Conference
on RF Power in Plasmas

Modeling Far-Field RF Sheaths in Alcator C-Mod

D. A. D'Ippolito[a], J. R. Myra[a], R. Ochoukov[b] and D. G. Whyte[b]

[a]*Lodestar Research Corporation, Boulder, CO, USA*
[b]*MIT Plasma Science and Fusion Center, Cambridge, MA, USA*

Abstract. It is shown that a theory of far-field sheath formation can qualitatively explain the observation on Alcator C-Mod of large plasma potentials (> 100 V) on field lines not directly connected to a powered antenna. The theory describes rf sheath formation when unabsorbed fast ICRF waves are incident on a conducting boundary possibly far away from the antenna. The resulting rf sheath drive is sensitive to the angle between the surface normal and the equilibrium B field. The main conclusion of this work is that the rapid tangential variation in the B field-limiter geometry at the tip of the limiter leads to the formation of large sheath potentials of the same order as the measured ones in C-Mod.

INTRODUCTION

RF sheath formation on antennas, walls and limiters is an important cause of reduced heating efficiency, local hot spots and impurity generation in ICRF-heated fusion experiments [1,2]. "Near-field" sheaths on field lines that connect directly to a powered antenna have been well studied. However, theory suggests that "far-field" sheaths on field lines that do not connect directly to a powered antenna can also be important [3-7]. This idea is indirectly supported by analyses of the origin and levels of impurities on many machines. Recent experiments on Alcator C-Mod have provided more direct evidence in the form of probe measurements of large plasma potentials on field lines that do not directly connect to the powered antennas [8,9] and thus are not due to near-field effects.

The radial profiles of the rf and ohmic potentials behind the limiter are shown in Fig. 1. The Ohmic potential is typically about 10 V and is constant in radius across the SOL. In the ICRF-heated case, the plasma potential is largest near the tip of the limiter and decays with radial distance from the tip. Its maximum value is about 400 V. The radial scale length at the tip (over which the angle between the B field and the limiter changes) is defined by d ~ 1 cm. In this paper, and in the more detailed account in [7], we show that sheath potentials > 100 V can be obtained using a 1D local far-field sheath model [6], and that the geometry of the limiter tip plays an important role in generating large potentials.

The reader is referred to [7] for more details on the modeling, and to [8,9] for more details of the diagnostics and the experimental data on electric fields and plasma potentials in the SOL and boundary region of Alcator C-Mod.
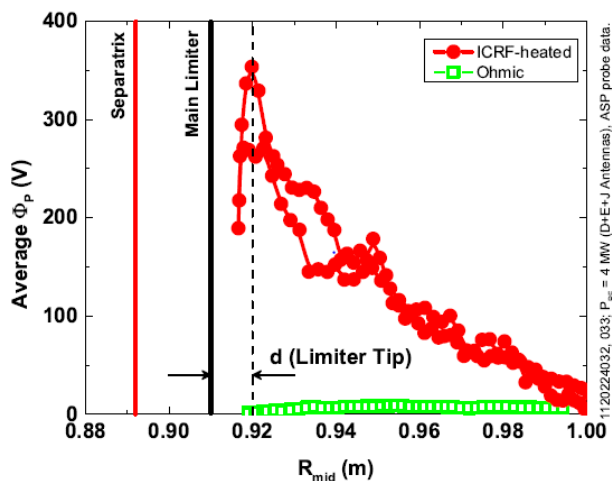
FIGURE 1. Radial variation of the plasma potential on Alcator C-Mod, measured by the A-port Scanning Probe and mapped to the midplane. Shown are the potential profiles in Ohmic (open squares) and ICRF-heated (filled circles) plasmas. The probe lies in the shadow of a limiter. © 2013 IOP Publishing. Reprinted from Ref. [7] by permission of IOP Publishing.

SHEATH MODEL

The starting point for the calculation is the far field sheath model in [6], slightly generalized as described below. It uses a wave-scattering formulation, with incoming and outgoing fast and slow waves coupled by an rf sheath BC at the sheath-plasma interface in the form

$$\mathbf{s} \times \mathbf{E} = \mathbf{s} \times \nabla(\Delta D_n) \quad , \tag{1}$$

where $\mathbf{s}$ is the unit vector normal to the sheath, Δ is the time-averaged sheath width, $D_n = \mathbf{s} \cdot \boldsymbol{\varepsilon} \cdot \mathbf{E}$, $\boldsymbol{\varepsilon}$ is the plasma dielectric and $\mathbf{E}$ is the total rf electric field summed over the four waves,

$$\mathbf{E} = e^{-i\omega t}\, e^{ik_y y}\, e^{ik_z z} \sum_{j=0}^{3} E_j \mathbf{e}_j\, e^{ik_{xj}x} \quad . \tag{2}$$

This model is one-dimensional (1D), varying in the direction normal to the sheath, and local to a particular contact point with the sheath. The rf field and plasma dielectric are evaluated on the plasma side of the sheath-plasma interface. We define the following local coordinate system: x denotes the direction normal to the sheath (with unit vector $\mathbf{s} = \hat{e}_x$) and (y, z) are the ignorable directions tangential to the sheath. The sheath is located at x = 0 and x > 0 is the plasma region.

We assume constant density near the boundary so that the 4th order dispersion relation can be solved algebraically, determining the index of refraction $\mathbf{n} = \mathbf{k}c/\omega$. For given values of n_y and n_z the dispersion relation is solved for the values of n_x of the coupled fast wave (FW) and slow wave (SW) roots. The wave structure in x is determined analytically by the sheath BC in Eq. (1). The solution for the wave amplitudes can be written in the form

$$E_1 = E_0 \frac{\mathbf{s} \cdot \mathbf{g}_2 \times \mathbf{g}_0}{\mathbf{s} \cdot \mathbf{g}_1 \times \mathbf{g}_2} + E_3 \frac{\mathbf{s} \cdot \mathbf{g}_2 \times \mathbf{g}_3}{\mathbf{s} \cdot \mathbf{g}_1 \times \mathbf{g}_2} \quad , \qquad E_2 = E_0 \frac{\mathbf{s} \cdot \mathbf{g}_0 \times \mathbf{g}_1}{\mathbf{s} \cdot \mathbf{g}_1 \times \mathbf{g}_2} + E_3 \frac{\mathbf{s} \cdot \mathbf{g}_3 \times \mathbf{g}_1}{\mathbf{s} \cdot \mathbf{g}_1 \times \mathbf{g}_2} \quad , \tag{3}$$

where $\mathbf{e}_j$ is the jth wave polarization vector [see Eq. (2)] and the vectors

$$\mathbf{g}_j = \mathbf{e}_j - i k_j \Delta (\mathbf{s} \cdot \boldsymbol{\varepsilon} \cdot \mathbf{e}_j) \tag{4}$$

contain an additional contribution from the sheath capacitance ($\propto \Delta$) term on the right hand side of the sheath BC (1). The subscripts 0 to 3 label the four roots of the dispersion relation. Rules are given in [6,7] for identifying each of these roots. For the case where the B field is nearly tangential to the boundary, the roots are ordered as follows: incident FW, reflected FW, reflected SW and incident SW. The naming convention for the FW and SW roots summarized here is the usual one when the roots are well separated, but breaks down when the B field is normal to the sheath. In that case the FW and SW solutions have similar scale lengths and what we choose to call the roots is somewhat arbitrary.

Given the field solution for all the waves, it is straightforward to calculate the instantaneous rf sheath potential and the rectified sheath potential

$$\Phi_{rf} \equiv \Delta \left| \sum_{j=0}^{3} \mathbf{s} \cdot \boldsymbol{\varepsilon} \cdot \mathbf{E}_j \right| \quad , \qquad \Phi_{sh} \approx 0.6\,\Phi_{rf} + 3T_e \quad . \tag{5}$$

We conclude this brief summary of the model by discussing two physics points. First, note that the vanishing of the denominator $\mathbf{s} \cdot \mathbf{g}_1 \times \mathbf{g}_2$ is associated with a *sheath-plasma wave (SPW) resonance* (see the discussions in [6,7]). This resonance occurs when the sheath width Δ and potential Φ_{rf} satisfy the Child-Langmuir (CL) constraint [10]. In the constrained model, the equations are non-linear, and multiple roots for the sheath potential are obtained in certain parameter regimes. The effects of this resonance for Alcator C-Mod parameters will be discussed below. Second, note that we use the *time-averaged* sheath width Δ in the sheath BC to determine the instantaneous rf field. Since the CL constraint involves only the rectified (DC) sheath potential, neglecting the oscillating part of the sheath width is a good lowest-order approximation.

NUMERICAL RESULTS

A key parameter in the far-field sheath model is the angle between the magnetic field line and the limiter surface, $\mathbf{s} \cdot \mathbf{b} \equiv b_x$. A key assumption of the model [7] is that the *rapid tangential variation* of this angle near the tip of the limiter provides the variation of the wave-fields along the surface and therefore an effective k_y, and that this large k_y can drive large sheath potentials. The base case parameters used here are B = 3.94 T, $n_e = 6 \times 10^{12}$ cm^{-3}, $T_e =$ 10 eV, charge state Z = 1, and mass ratio $m_i/m_p = 2$ (deuterium). The ICRF frequency and power are f = 80 MHz, and P_{ICRF} = 4 MW. We assume a FW amplitude in the range E_{rf} = 6 - 22 V/cm. (The lower bound is inferred from a direct measurement by a B-dot probe in the limiter shadow, and the upper bound is obtained from a Poynting flux argument assuming that 5% of the ICRF power is unabsorbed in the core and uniformly spread around the SOL). Unless stated otherwise, the index of refraction in the tangential directions is assumed to be in the range $n_y = k_y c/\omega = 60 - 100$, where $k_y \sim 1/d$ to π/d and d = 1 cm.

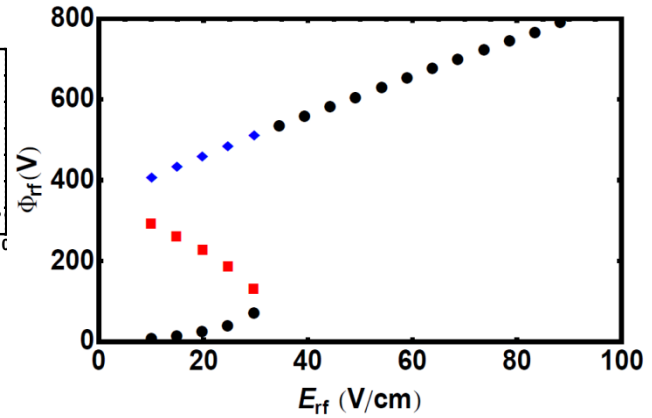For the base case parameters, the computed sheath potential Φ_{rf} increases with b_x [7]. For a fixed large value of n_y, a small (large) sheath potential is obtained when the magnetic field line is nearly tangential (normal) to the sheath. Applied to tokamak limiter geometry, this means that the plasma potential will be small in the main SOL and rapidly increase with major radius in the private SOL behind the limiter tip, until the point is reached where the B field is normal to the flat side of the limiter. This prediction agrees with the data (see Fig. 1). In the rest of this section we set b_x = 1.
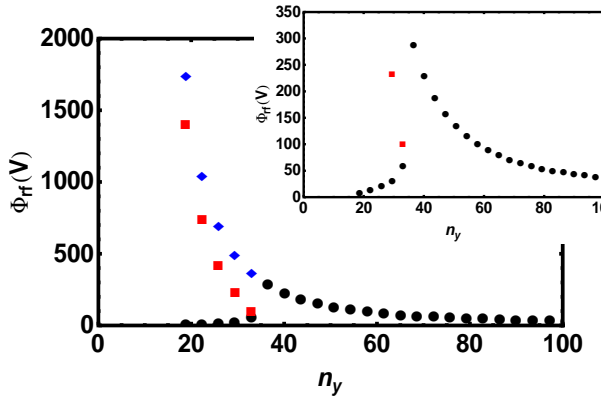
FIGURE 2. Dependence of the far-field rf sheath potential Φ_{rf} on the tangential index of refraction n_y for the base case parameters with E_{rf} = 22 V/cm and b_x = 1. © 2013 IOP Publishing. Reprinted from Ref. [7] by permission of IOP Publishing.

FIGURE 3. Dependence of the far-field rf sheath potential Φ_{rf} on the local FW electric field E_{rf} for the base case parameters with n_y = 30 and b_x = 1. © 2013 IOP Publishing. Reprinted from Ref. [7] by permission of IOP Publishing.

Figure 2 shows the solution for the rf sheath potential as a function of the tangential component of the index of refraction, $n_y = k_y c/\omega$, which we assume is determined by the magnetic field and limiter geometry as just described. Note that there is a SPW resonance that produces three roots. The inset shows a blow-up of the solution near the resonance. For the base case parameters (e.g. n_y = 60) the sheath potential is about 100 V and rises rapidly as the resonance is approached. The nonlinearity that produces multiple roots is caused by the Child-Langmuir constraint relating the DC sheath width Δ to the rf sheath voltage.

Figure 3 shows that there is also a resonance in the dependence of Φ_{rf} on the rf electric field. Following the lowest root (denoted by black filled circles), we find a jump in the sheath potential at around E_{rf} = 30 V/ cm. The existence of a sharp threshold vs electric field is also found in the data [8,9].

As discussed in [7] and in some of our earlier papers [6,11], it is useful to define a parameter Λ measuring the effect of the sheath capacitance in the rf sheath BC. We define $\Lambda \equiv k_\parallel \Delta \varepsilon_\parallel$ (electrostatic limit) or $\Lambda \equiv k_\parallel \Delta n_\perp^2$ (general electromagnetic case), where $n_\perp^2$ is from the SW root. When $\Lambda \sim 1$ the two terms in the rf sheath BC are comparable in magnitude, and the nonlinearity of the sheath BC becomes important for $\Lambda > 1$. As shown in Figs. 2 and 3, the nonlinear regime has a region of parameter space where there are three roots and a threshold for greatly enhanced rf-sheath potential. The resonance point corresponds to $\Lambda \sim 1$ (to within a factor of 2).

CONCLUSIONS

The Alcator C-Mod data analyzed here provides the first direct experimental test of our far-field sheath theory [6]. Since the present model is 1D and local to a single point on the sheath, the comparison is only qualitative. The theoretical model allows the fast wave to couple to slow waves, which in turn generate large sheath potentials. It was found that a key element in obtaining large potentials is the rapid tangential variation of the angle between the magnetic field line and the normal to the limiter surface. This is a likely explanation for the origin of the plasma potential in areas that do not map to powered antennas.

The following points of agreement are found between the Alcator C-Mod experimental data [8,9] on SOL plasma potentials and the far field sheath model [6,7]:

(a) Large rf-induced sheath potentials (~ 100 V) are obtained on field lines which do not pass near a powered antenna but are near the tip of the poloidal limiter; the magnitude and the radial location of the sheath potentials in the model and experiment are in rough agreement.

(b) There is a FW intensity threshold for obtaining large sheath potentials. In the present model, it corresponds physically to the limit $\Lambda \equiv k_\parallel \Delta n_\perp^2 > 1$ in which the sheath capacitance term in the sheath BC exceeds the vacuum term.

This work impacts the important problem of impurity generation. Enhanced sputtering due to ions accelerated by the rf sheaths [12] is an important mechanism to explain rf-enhanced impurity sources both near and far from the ICRF antennas. In the present case, FW far-field sheath theory provides a possible explanation for the origin of the increased Mo sources from limiter surfaces observed during ICRF on Alcator C-Mod.

ACKNOWLEDGMENTS

REFERENCES

1. J.-M. Noterdaeme and G. Van Oost, Plasma Phys. Control. Fusion **35**, 1481 (1993).
2. J. R. Myra, D. A. D'Ippolito, D. A. Russell, L. A. Berry, E. F. Jaeger and M. D. Carter, Nucl. Fusion **46**, S455 (2006).
3. F. W. Perkins, Bull. Am. Phys. Soc. **34**, 2093 (1989).
4. M. Brambilla, R. Chodura, J. Hoffmann, and J. Neuhauser, *Plasma Phys. Control. Nucl. Fusion Res. 1990* (IAEA, Vienna, 1991), Vol. **1**, p. 723.
5. J. R. Myra, D. A. D'Ippolito and M. Bures, Phys. Plasmas **1**, 2890 (1994).
6. D. A. D'Ippolito, J. R. Myra, E. F. Jaeger and L. A. Berry, Phys. Plasmas **15**, 102501 (2008).
7. D. A. D'Ippolito, J. R. Myra, R. Ochoukov and D. G. Whyte, Plasma Physics Control. Fusion **55**, 085001 (2013).
8. R. Ochoukov, D.G. Whyte, D. Brunner, I. Cziegler, B. LaBombard, B. Lipschultz, J. Myra, J. Terry, and S. Wukitch, to be published in J. Nucl. Mater. (2013); http://dx.doi.org/10.1016/j.jnucmat.2013.01.189.
9. R. Ochoukov, D.G. Whyte, D. Brunner, D.A. D'Ippolito, B. LaBombard, B. Lipschultz, J.R. Myra, J.L. Terry, S.J. Wukitch, submitted to Plasma Phys. Control. Fusion (2013).
10. C. D. Child, Phys. Rev. (Series I) **32**, 492 (1911); I. Langmuir Phys. Rev**. 21**, 419 (1923).
11. J. R. Myra and D. A. D'Ippolito, Plasma Phys. Control. Fusion **52**, 015003 (2010).
12. D. A. D'Ippolito, J. R. Myra, M. Bures and J. Jacquinot, Plasma Phys. and Controlled Fusion **33**, 607 (1991).